ELSEVIER

Journal of Molecular Catalysis A: Chemical 168 (2001) 289–297

JOURNAL OF MOLECULAR CATALYSIS A: CHEMICAL

www.elsevier.com/locate/molcata

Substitution effects of In^{3+} by Fe^{3+} on photocatalytic and structural properties of Bi_2InNbO_7 photocatalysts

Zhigang Zou [a], Jinhua Ye [b], Hironori Arakawa [a,*]

[a] *National Institute of Materials and Chemical Research, 1-1 Higashi, Tsukuba, Ibaraki 305, Japan*
[b] *National Research Institute for Metals, 1-2-1 Sengen, Tsukuba, Ibaraki 305, Japan*

Received 1 August 2000; received in revised form 23 November 2000; accepted 23 November 2000

Abstract

The substitution effect of In^{3+} by Fe^{3+} on photocatalytic and structural properties of Bi_2InNbO_7 photocatalysts was investigated. The new photocatalysts, Bi_2MNbO_7 ($M = Fe^{3+}$, In^{3+}), were synthesized by the solid-state reaction and characterized by powder X-ray diffraction and Rietveld structure refinement. Bi_2MNbO_7 ($M = Fe^{3+}$, In^{3+}) crystallize in the same pyrochlore structure, but the lattice parameters decrease with In^{3+} being substituted by Fe^{3+}. The formation rates of H_2 and O_2 evolutions from an aqueous methanol and a cerium sulfate solution, respectively, increase significantly with In^{3+} being substituted by Fe^{3+} under UV irradiation. The H_2 evolution was obtained from pure H_2O under UV irradiation with the Bi_2MNbO_7 ($M = Fe^{3+}$, In^{3+}) catalyst without co-catalyst such as Pt. The formation rate of H_2 evolution increases with In^{3+} being substituted by Fe^{3+}. The Bi_2FeNbO_7 photocatalyst exhibits much higher photocatalytic activity than the well-known TiO_2 photocatalyst in pure water. © 2001 Published by Elsevier Science B.V.

Keywords: Bi_2MNbO_7 ($M = Fe^{3+}$, In^{3+}); Solid-state reaction; Photocatalyst; Substitution effect

1. Introduction

The study of photocatalytic water splitting has attracted much interest, since it can be a promising chemical route for energy renewal and storage [1–5]. However, the number of photocatalysts known up to now is yet limited, and the activity is still low. Therefore, it is in urgent need to develop new type of photocatalyst with higher activity [6,7]. The process of photocatalytic reaction of oxides is explained generally that the photon is absorbed directly by band gap of the conventional semiconductor, generating electron-hole pair in the conduction band and the valence band, respectively [8]. Such studies are often related to electron transfer and energy transfer processes in photocatalytic reactions [9–11].

Very recently, we have found that Bi_2InNbO_7 shows semiconducting behavior. Furthermore, we found that Bi_2InNbO_7 acts as a photocatalyst under UV irradiation [12]. The compound has band gap of about 2.7 eV and seems to have potential to improve its activity by modifying the structure [12]. We suggest that substitution of In^{3+} by Fe^{3+} in Bi_2InNbO_7 might cause a slight modification of crystal structure, resulting in a change in photocatalytic and photophysical properties [12]. It is known that a slight modification of structure to semiconductor has a dramatic effect on the physical properties [13]. The change of lattice constants might lead to hole/electron delocalization [13]. However, the improvement in mobility of the charge is important

* Corresponding author. Tel.: +81-298-61-4410; fax: +81-298-61-4524.
E-mail address: h.arakawa@home.nimc.go.jp (H. Arakawa).

1381-1169/01/$ – see front matter © 2001 Published by Elsevier Science B.V.
PII: S1381-1169(00)00545-8

to photocatalysts because it affects the probability of electrons to reach reaction sites on the surface of photocatalyst.

Here we report the preparation, photocatalytic and structural characterizations of the Bi_2MNbO_7 (M^{3+} = Fe^{3+}, In^{3+}) photocatalysts. A comparison of the photocatalytic property of Bi_2MNbO_7 (M^{3+} = Fe^{3+}, In^{3+}) with the TiO_2 photocatalyst is presented.

2. Experimental

2.1. Preparation of photocatalysts and characterization

The polycrystalline samples of the Bi_2MNbO_7 (M^{3+} = Fe^{3+}, In^{3+}) photocatalysts were prepared by solid state reaction method. The high purity chemicals of In_2O_3, α-Fe_2O_3, $Bi_2(CO_3)_3$ and Nb_2O_5 were used as starting materials. M_2O_3 (M^{3+} = Fe^{3+}, In^{3+}) was dried at 700°C and Nb_2O_5 at 600°C before syntheses. The stoichiometric amounts of precursors were mixed and pressed into small columns. The small columns were sintered in an alumina crucible using an electric furnace. In order to investigate the best conditions for sintering temperature, the small columns were calcined at different reaction temperature, and the sintered products were analyzed by powder X-ray diffraction. The result of X-ray diffraction showed that with increasing reaction temperature the impurities decreased rapidly. The powder X-ray diffraction analysis revealed that the product could be melted when sintering temperature was over 1080°C. Therefore, the sintering temperature was selected at 1080°C for Bi_2FeNbO_7. The sintered sample was ground and re-pressed into small columns after heating. The same procedure was performed three times for the samples. At the final process, the pressed columns were reacted for two more days at 1080°C, producing pure phase. We found that this method is easy to obtain a pure phase. The Bi_2InNbO_7 photocatalyst was prepared at 1100°C as the same method [12].

The chemical composition of the photocatalysts before and after photocatalytic reactions was determined by scanning electron microscope–X-ray energy dispersion spectrum (SEM–EDS) with accelerating voltage of 25 kV. The structural properties of the photocatalysts were investigated by powder X-ray diffraction method (Rigaku RINT-2000 diffractometer using Cu Kα radiation (λ = 1.54178 Å)). In order to detect the oxygen on surface. Magnetic susceptibility measurement was performed in the temperature range 5–300 K and at an applied filed of 1.0 T using a Superconducting Quantum Interference Device (SQUID) magnetometer. UV–VIS diffuse reflectance spectrum of the photocatalysts was measured by using an UV–VIS spectrometer. The surface area was determined by BET measurement.

2.2. Photocatalytic reaction

The photocatalytic reaction was examined using a closed gas circulation system and an inner-irradiation type with quartz cooling cell and a 400 W high-pressure Hg lamp. The gases evolved were determined with TCD gas chromatograph, which was connected with a circulating line. In order to obtain high activity, it is essential to load a metal or metal oxide on the surface of photocatalyst. Pt was found to be the most effective for the TiO_2 photocatalyst [4,9]. The photocatalytic reaction was performed in an aqueous CH_3OH/H_2O solution (1.0 g of 0.1 wt.% Pt load powder catalyst, 50 ml CH_3OH, 350 ml H_2O) and in pure water (1.0 g powder catalyst without co-catalyst such as Pt, 400 ml H_2O). O_2 evolution reaction was performed in an aqueous cerium sulfate solution (1.0 g powder catalyst, 1.0 mmol $Ce(SO_4)_2$, 400 ml H_2O) since the solution is more stable than an aqueous silver nitrate under UV irradiation [14]. In order to check photocatalytic activity of Pt itself, the 1.0 wt.% Pt/SiO_2 sample was prepared and was tested by the same method as used for Bi_2MNbO_7 (M = Fe^{3+}, In^{3+}). Pt was loaded on surface of SiO_2 by H_2 reaction method at 300°C for 2 h.

3. Results

3.1. Structural and physical properties

Powder X-ray diffraction data were collected with a step scan procedure in the range of 2θ = 5–100°. The diffraction patterns indicate that each of the Bi_2MNbO_7 (M^{3+} = Fe^{3+}, In^{3+}) compounds is a single phase. This is consistent with the observation from SEM–EDS. Full-profile structure refinement of

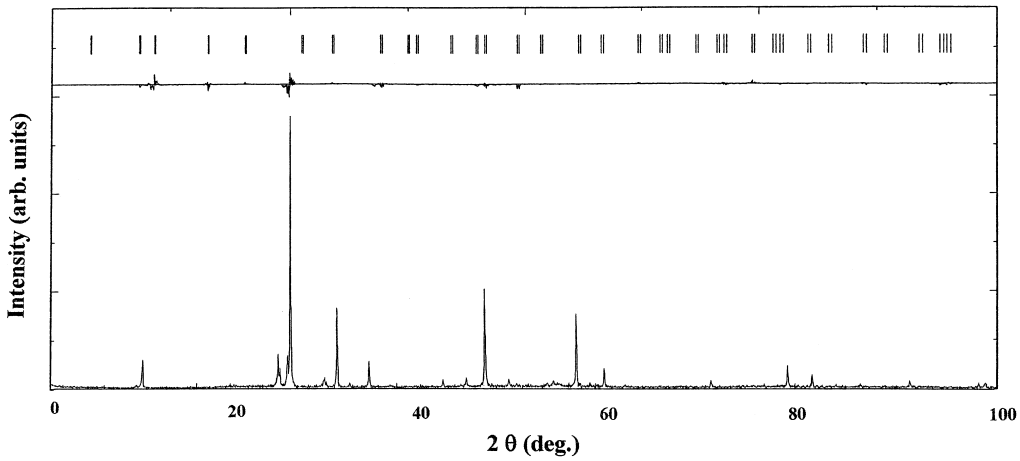

Fig. 1. The result of refinement for powder X-ray diffraction data of Bi_2FeNbO_7.

the collected powder diffraction data was performed using the Rietveld program REITAN [15]. Positional parameters and isotropic thermal parameters of the photocatalysts were refined. Fig. 1 shows a typical result of refinement for Bi_2FeNbO_7, indicating a good agreement between the observed and calculated intensities in the pyrochlore structure [12]. The outcome of the final refinement indicated that the Bi_2MNbO_7 (M^{3+} = Fe^{3+}, In^{3+}) photocatalysts crystallize in the same structure, cubic system with space group *Fd3m*. 2θ angles of each reflection, however, changed with In^{3+} being substituted by Fe^{3+}, indicating a decrease in lattice parameter of the compounds with decrease of the M^{3+} ionic radii, Fe^{3+}(0.67 Å) ≪ In^{3+} (0.92 Å). The lattice parameters decrease from a = 10.7793(2) Å for Bi_2InNbO_7 to a = 10.5233(2) Å for Bi_2FeNbO_7. All the diffraction peaks for the Bi_2MNbO_7 (M^{3+} = Fe^{3+}, In^{3+}) photocatalysts could be indexed based on the lattice parameters and the space group mentioned above.

Table 1 shows the physical properties of the photocatalysts. BET measurement showed that the surface areas of Bi_2MNbO_7 (M^{3+} = Fe^{3+}, In^{3+}) are 0.48 and 0.52 $m^2\,g^{-1}$, respectively. This is about 1% of the value in TiO_2 photocatalyst (53.8 $m^2\,g^{-1}$). This means that surface area of Bi_2MNbO_7 (M^{3+} = Fe^{3+}, In^{3+}) is much smaller than that of TiO_2 photocatalyst.

Fig. 2 shows the result of diffuse reflection spectra. The onset of diffuse reflection spectra of these photocatalysts showed an obvious shift to longer wavelength with In^{3+} being substituted by Fe^{3+}. The band gaps of the Bi_2MNbO_7 (M^{3+} = Fe^{3+} and In^{3+}) photocatalysts were estimated to be about 2.2 and 2.7 eV from onset of diffuse reflection spectra as shown in

Table 1
Rates of gas evolution and physical properties of photocatalysts

Catalyst	Type of structure	Lattice parameter a (Å)[a]	Band gap (eV)	Surface area ($m^2\,g^{-1}$)	Rate of gas evolutions (μ mol h^{-1})			
					CH_3OH/H_2O[b]		$Ce(SO_4)_2/H_2O$[c]	Pure H_2O[c]
					H_2	CO	O_2	H_2
Bi_2FeNbO_7	Pyrochlore	10.5233 (2)	2.2	0.48	600	24	102	8.0
Bi_2InNbO_7	Pyrochlore	10.7793 (2)	2.7	0.52	180	5	10	1.5
TiO_2 (TiO_2-P25)	Anatase + rutile		3.2	53.8	560	15	22	1.0

[a] The cubic system with space group *Fd3m* was obtained by Rietveld refinement.
[b] Pt (0.1 wt.%) was loaded on the surface of powder catalyst.
[c] Without co-catalyst was used such as Pt.

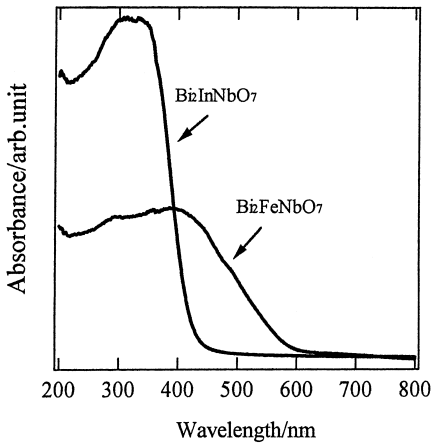

Fig. 2. UV–VIS diffuse reflectance spectrums of Bi_2MNbO_7 ($M^{3+} = Fe^{3+}$, In^{3+}).

Table 1, respectively. This means that the band gap decreases with a decrease of M^{3+} ionic radii.

3.2. Photocatalytic activity in aqueous solution and pure water

Fig. 3 shows the H_2 evolution from CH_3OH/H_2O solution under UV irradiation with the Pt/Bi_2MNbO_7 ($M^{3+} = Fe^{3+}$, In^{3+}) photocatalysts. The formation rate of H_2 increased significantly with In^{3+} being substituted by Fe^{3+}. This means that the activity of these photocatalysts increases with In^{3+} being substituted by Fe^{3+}. The formation rate of H_2 was estimated to be 0.6 and 0.18 mmol g^{-1} h^{-1} during the first 10 h, respectively. The total amount of H_2/catalyst (mol) for these compounds was much greater than 1.0 after 10 h, indicating that the reaction seems to occur catalytically. The reaction stopped when the light was turned off in this experiment, showing the obvious light response. The result shows that the photocatalytic reaction is induced by the absorption of UV irradiation. It is notable that the formation rate of H_2 evolution for Pt/Bi_2FeNbO_7 is slightly larger than that of Pt/TiO_2 photocatalyst (TiO_2-P25). This means that the activity of Pt/Bi_2FeNbO_7 is higher than that of Pt/TiO_2 photocatalyst. The effect of co-catalyst Pt on photocatalytic activity was investigated by the same condition. The result showed that the formation rate of H_2 on 1.0 wt.% Pt/SiO_2 sample was much lower than that on the Pt/TiO_2 and Pt/Bi_2MNbO_7 ($M^{3+} = Fe^{3+}$, In^{3+}) photocatalysts. This means that the co-catalyst Pt has very little effect to this photocatalytic reaction.

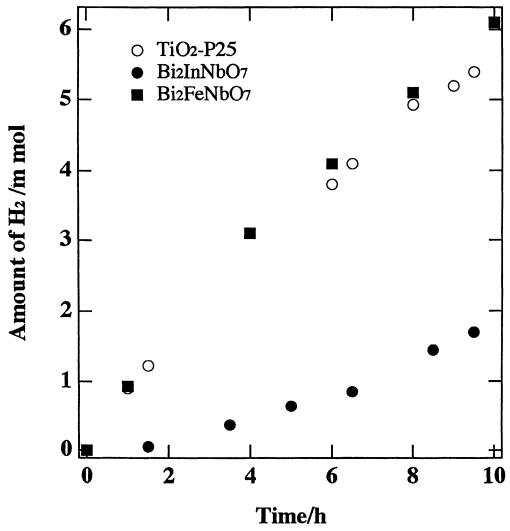

Fig. 3. Photocatalytic H_2 evolutions over Pt/Bi_2MNbO_7 ($M^{3+} = Fe^{3+}$, In^{3+}) and Pt/TiO_2 (TiO_2-P25) from CH_3OH/H_2O solution under UV irradiation. Catalyst: 1.0 g; CH_3OH: 50 ml; H_2O: 350 ml, 400 W high-pressure Hg lamp.

The CO evolutions were observed in this reaction from CH_3OH/H_2O solution as the oxidation product [12]. The result is shown in Table 1. The CO evolution increased significantly with In^{3+} being substituted by Fe^{3+}, as does H_2 evolution. However, the rate of CO evolution is much lower than that of H_2 evolution. It is well known that when CH_3OH is added to a Pt/TiO_2 aqueous suspension, sustained H_2 production is observed under UV irradiation and the alcohol molecules are oxidized to final productions of CO_2, CO, CH_4 [5]. We suggest that phenomenon observed over Pt/TiO_2 also takes place in our photocatalysts.

O_2 evolution reaction was performed in an aqueous cerium sulfate solution and the following stoichiometric reaction took place

$$4Ce^{4+} + 2H_2O \rightarrow 4Ce^{3+} + O_2 + 4H^+$$

Fig. 4 shows the formation rate of O_2 evolutions from aqueous $Ce(SO_4)_2$ solution under UV irradiation with the Bi_2MNbO_7 ($M^{3+} = Fe^{3+}$, In^{3+}) photocatalysts. The aqueous $Ce(SO_4)_2$ solution is more stable than an aqueous silver nitrate under UV irradiation since photodeposition of Ce^{3+} does not occur after illumination [14]. The formation rate of O_2 evolution in the

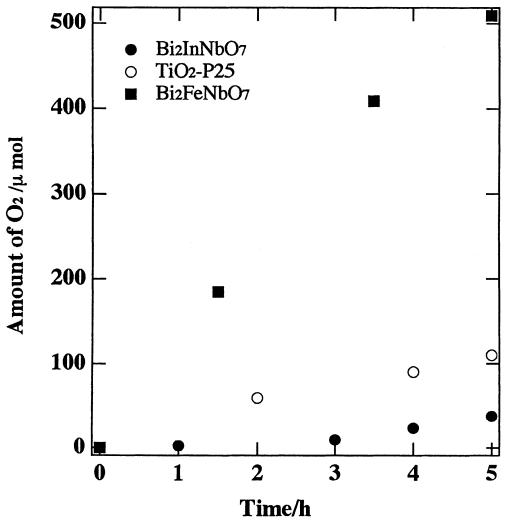

Fig. 4. Photocatalytic O_2 evolutions on Bi_2MNbO_7 ($M^{3+} = Fe^{3+}$, In^{3+}) and TiO_2 (TiO_2-P25) from an aqueous cerium sulfate solution under UV irradiation. Catalyst: 1.0 g; $Ce(SO_4)_2$: 1.0 mmol; H_2O: 400 ml, 400 W high-pressure Hg lamp.

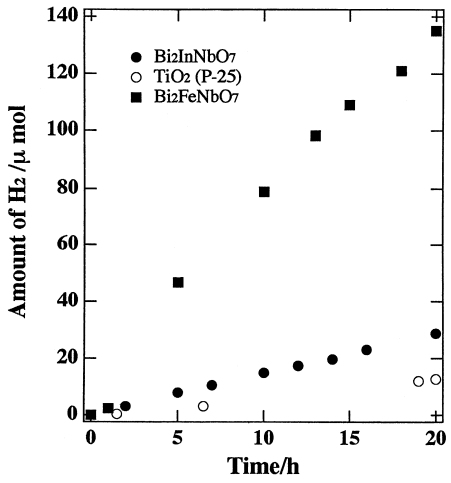

Fig. 5. Photocatalytic H_2 evolutions on Bi_2MNbO_7 ($M^{3+} = Fe^{3+}$, In^{3+}) and TiO_2 (TiO_2-P25) from pure water without co-catalyst Pt and CH_3OH under UV irradiation. Catalyst: 1.0 g; H_2O: 400 ml, 400 W high-pressure Hg lamp.

first 5 h increased rapidly with decrease of M^{3+} ionic radii in a similar manner as H_2 evolution. This means that the photocatalysts have potentials for O_2 evolution from aqueous solution and the potential activity for O_2 evolutions increase with decrease of M^{3+} ionic radii. It is interesting to notice that the formation rate of O_2 evolution on Bi_2FeNbO_7 is much larger than that on the TiO_2 photocatalyst. This means that the activity of Bi_2FeNbO_7 is much higher than that of the TiO_2 photocatalyst.

Fig. 5 shows the H_2 evolution using the TiO_2 and Bi_2MNbO_7 ($M^{3+} = Fe^{3+}$, In^{3+}) photocatalysts from pure water without co-catalyst Pt and CH_3OH under UV irradiation. The formation rates of H_2 evolution with the Bi_2MNbO_7 ($M^{3+} = Fe^{3+}$, In^{3+}) photocatalysts were about 8.0 and 1.5 mmol g^{-1} h^{-1} in the first 10 h, respectively. TiO_2 photocatalyst (TiO_2-P25) was tested by the same method. The formation rate of H_2 evolution was about 1.0 mmol h^{-1} for the first 10 h. The TiO_2 photocatalyst shows much lower activity than that of the Bi_2FeNbO_7 photocatalyst, even lower than that of the Bi_2InNbO_7 photocatalyst in pure water. This means that although the TiO_2 photocatalyst showed very high photocatalytic activity under UV light irradiation in an aqueous CH_3OH/H_2O solution, photocatalytic activity is very low in pure water. Oxygen evolution was not observed from pure water in this experiment using both of Bi_2MNbO_7 ($M^{3+} = Fe^{3+}$, In^{3+}) and TiO_2. The reason will be discussed hereafter.

4. Discussion

4.1. Effects of crystal and band structures on photocatalytic activity

The detailed investigations on structure found that the three-dimensional network of octahedral MO_6 (M = Fe3+, In^{3+} and Nb^{5+}) in crystal structure of Bi_2MNbO_7 ($M^{3+} = Fe^{3+}$, In^{3+}) are stacked along [0 0 1]. Fig. 6 shows the schematic structural diagram of Bi_2MNbO_7 ($M^{3+} = Fe^{3+}$, In^{3+}). This is consistent with the relatively smaller resistivity in this direction from conductivity measurement [12]. Conductivity measurement suggests that electron-hole pairs in Bi_2InNbO_7 can move easily in this direction [12]. Change of lattice parameters might led to a modification of the zigzag chains, which improves mobility of the charge [13]. Conductivity measurement of Bi2InNbO7 showed that electron-hole pairs in Bi_2InNbO_7 are to be movement along [0 0 1], the zigzag chains [12]. The mobility of electron-hole pairs affects the photocatalysis because it affects the

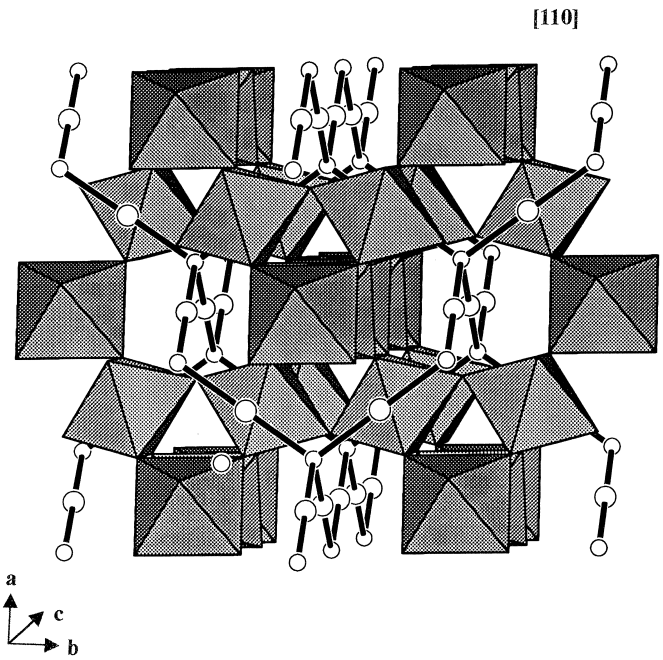

Fig. 6. The schematic structural diagram of Bi_2MNbO_7 (M^{3+} = Fe^{3+}, In^{3+}). Three-dimensional network of MO_6 stacked along [0 0 1] and separated by a unit cell translation.

probability of electrons and holes to reach reaction sites on the surface of photocatalyst. This suggests that although both Bi_2FeNbO_7 and Bi_2InNbO_7 have similar structure, the movement of electrons might be more easily in Bi_2FeNbO_7 than that in Bi_2InNbO_7. Kudo et al. found similar results from study of the photocatalytic activity of the perovskite structure, $Sr_2Ta_2O_7$ and $Sr_2Nb_2O_7$, which consists of MO_6 (M = Nb, Ta) octahedron. The MO_6 (M = Nb, Ta) octahedrons form a zigzag chains. $Sr_2Ta_2O_7$ and $Sr_2Nb_2O_7$ crystallize in the same perovskite structure, but the lattice parameters are different. They found that the bond angle of O–Ta–O in $Sr_2Ta_2O_7$ is close to an ideal pervoskite structure, while the connection of octahedron in $Sr_2Nb_2O_7$ is twisted. The photocatalytic activity of $Sr_2Ta_2O_7$ is higher than that of $Sr_2Nb_2O_7$ because the photogenerated electron-hole pairs in $Sr_2Ta_2O_7$ can move more easily than those in $Sr_2Nb_2O_7$ [11].

The band structure of oxides is generally defined by M d-level and O 2p-level. Scaife examined that the valence band energy should be assumed by the O 2p-levels in MO_6 and the conduction band assumed by d-levels in MO_6 when the compound contains octahedral MO_6 [16]. The band gaps of Bi_2MNbO_7 (M^{3+} = Fe^{3+}, In^{3+}) decreased from 2.7 eV for Bi_2InNbO_7 to 2.2 eV for Bi_2FeNbO_7 with In^{3+} being substituted by Fe^{3+}. The difference of band gaps in the photocatalysts might result from that of conduction band. The valence band potentials of the Bi_2MNbO_7 (M^{3+} = Fe^{3+}, In^{3+}) photocatalysts should be the same because they have same crystal structure. The conduction band potentials of the photocatalysts might be changed because the difference of octahedrons in the Bi_2MNbO_7 (M^{3+} = Fe^{3+}, In^{3+}) photocatalysts. The conduction bands of Bi_2MNbO_7 (M^{3+} = Fe^{3+}, In^{3+}) should be slightly changed towards negative with In^{3+} being substituted by Fe^{3+} since the band gaps of Bi_2MNbO_7 (M^{3+} = Fe^{3+}, In^{3+}) decrease with In^{3+} being substituted by Fe^{3+}.

The difference in the surface area of the photocatalysts can generally lead to the difference in photocatalytic activity since an efficient photocatalytic reaction process occurs on the photocatalyst surface. As Table 1, Bi_2InNbO_7 and Bi_2FeNbO_7 have very similar surface area; hence the difference

photocatalytic activity cannot be attributed to variations in surface area. The fact suggests the difference in the photocatalytic activity may be mainly due to their different band structure.

It is interesting to notice that Bi_2MNbO_7 (M^{3+} = Fe^{3+}, In^{3+}) show photoabsorption in the visible light region ($\lambda > 420$ nm) (see Fig. 2). This means that the photocatalysts have ability to respond wavelength of visible light region. However, H_2 and O_2 were not evolved using the Bi_2MNbO_7 (M^{3+} = Fe^{3+}, In^{3+}) photocatalyst from CH_3OH/H_2O and $Ce(SO_4)_2/H_2O$ solutions, respectively. Alig et al. [17] has shown that direct absorption of photons by band gap of oxides can generate electron-hole pairs in a solid. However, the energy of requirement is generally higher than the band gap of the oxides [18,19]. Considering the fact that in the process of splitting water into H_2 and O_2 by photocatalysis, four holes and two electrons are necessary on surface of the photocatalysts at least. This suggests that larger energy than the band gap of photocatalysts seems to be necessary to photocatalytic splitting of water. In order to obtain high activity, two approaches are possible. One way would be to further modify the catalyst surface to increase the range of wavelengths at which the catalyst is active. Another would be to increase the irradiation energy.

BET measurement showed that the surface areas of Bi_2MNbO_7 (M^{3+} = Fe^{3+}, In^{3+}) are about 1% of that of TiO_2 photocatalyst. Since an efficient photocatalytic reaction process occurs on the photocatalyst surface, the smaller surface area of the Bi_2MNbO_7 (M^{3+} = Fe^{3+}, In^{3+}) photocatalysts might lead to low activity of the photocatalytic reaction. The study for effects of surface area on effective photocatalytic reaction and on range of responding wavelength is in progress, which is believed to further understand the new photocatalysts.

4.2. Photooxidation/photodissolution of photocatalysts and photoadsorption of oxygen

It is known that the photooxidation/photodissolution of catalyst might consume oxygen. However, such a kind of reaction generally leads to the changes in crystal structure and the chemical composition of photocatalyst. We examined the atomic ratio and the crystal structure of Bi_2MNbO_7 (M^{3+} = Fe^{3+}, In^{3+}) before and after photocatalytic reactions.

The chemical composition of these photocatalysts was determined by SEM–EDS analysis. The composition content was decided using the ZAF (*Z*: element number("*Z*" number) correction; *A*: absorption correction; *F*: fluorescence correction) quantification method. SEM–EDS analysis revealed that the chemical component of the Bi_2MNbO_7 (M^{3+} = Fe^{3+}, In^{3+}) compounds is close to stoichiometry. These photocatalysts have a homogenous atomic distribution with no other additional elements. The atomic ratio of these photocatalysts was confirmed by X-ray fluorescence spectrometer (XRFS) measurement. The observation is in agreement with results of SEM–EDS analysis. Oxygen content was calculated from the EDS results [13].

The crystal structure of the photocatalysts before and after photocatalytic reactions was investigated using X-ray powder diffraction. The result is shown in Fig. 1. From these experimental results we confirmed that these samples before and after reactions have not changed in both the crystal structure and the chemical composition.

Oxygen evolution was not observed from pure water in this experiment using both the Bi_2MNbO_7 (M^{3+} = Fe^{3+}, In^{3+}) and the TiO_2 photocatalysts. It is commonly accepted that free holes in TiO_2 particles can generate OH radicals either on the surface or even at the aqueous interface [20,21]. Extensive research found that there are both the physisorbed and chemisorbed oxygen molecules on TiO_2 surface by low-energy photon irradiation [22,23]. The physisorbed O_2 molecules are produced through the neutralization of chemisorbed O_2^- species by photo-generated holes. Amy et al. found also similar result in TiO_2 photocatalyst that the produced oxygen can be photoadsorbed on the surface of photocatalyst [24]. Very recently, Ishibashi et al. found that under UV light illumination O_2^- was formed on the order of 10^{14} cm^{-2} at the TiO_2 surface during photocatalytic reaction. This indicates photogenerated electron is mainly trapped by adsorbed oxygen resulting in the formation of O_2^- [25].

The photoadsorption of oxygen on the photocatalysts after photocatalytic reaction in pure water was investigated by measurements of magnetic susceptibility (χ/T). The magnetic susceptibility of oxygen adsorbed on solid surface was studied by many authors and it was shown that adsorbed oxygen

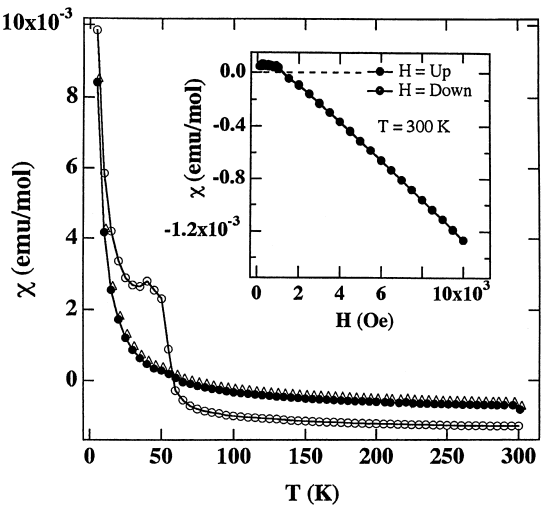

Fig. 7. A comparison of magnetic susceptibility for Bi_2InNbO_7 before and after photocatalytic reactions: (●) before photocatalytic reactions; (○) after photocatalytic reactions; (△) sintered; inset: the variation of χ as a function of magnetic filed at 300 K (χ/H).

undergoes an antiferromagntic transition around 50 K [26,27]. Fig. 7 shows a comparison of magnetic susceptibility for Bi_2InNbO_7 before and after photocatalytic reactions. The inset shows the variation of χ as a function of magnetic filed at 300 K (χ/H). The susceptibility at low temperature is different between two samples before and after reactions. The magnetic susceptibility of photocatalyst before reaction in the temperature range could be fit to a modified Curie–Weiss relation according to the equation, $\chi = \chi_0 + C/(T + \Theta)$, where χ_0 is temperature-independent contributions such as Van Vleck and Pauli magnetism, C the Curie constant, and Θ denotes the Curie–Weiss temperature [28]. The sample after reaction shows an obvious broad peak around 50 K. Measurements under zero field and field cooled conditions revealed that the susceptibility is independent to the applied magnetic field. The fact suggests that the origin of this anomaly is unlikely from a spin-glass-like behavior. To understand further the origin of this anomaly, the sample after reaction was sintered at 600°C using an electric furnace to deoxidation. The sintered sample showed the same result as that of sample before reaction(see Fig. 9), the broad peak around 50 K disappeared after sintering. The anomaly seen around 50 K might arises from the antiferromagnetic ordering of adsorbed oxygen in the sample. The similar result was also observed in other compounds of containing niobium, such as in $K_7Nb_{14.13}P_{8.87}O_{60}$ and $BaNb_2S_5$ [29–31]. Although it is not clear whether the O_2 molecule photoadsorbed on surface of the photocatalysts is physisorbed and/or chemisorbed molecule states, we speculate that the phenomenon observed in TiO_2 also takes place on the surface of our photocatalysts. Further study of the photoadsorption of oxygen on these samples under UV irradiation is in progress, which is believed to supply more concrete information.

5. Conclusions

The photocatalysts, Bi_2MNbO_7 (M^{3+} = Fe^{3+}, In^{3+}), were synthesized by the solid-state reaction. The experimental results show that Bi_2MNbO_7 (M^{3+} = Fe^{3+}, In^{3+}) are sensitive to UV irradiation and that it is possible to obtain H_2 from both CH_3OH/H_2O solution and pure water, and to obtain O_2 from an aqueous cerium sulfate solution. Although Bi_2MNbO_7 (M^{3+} = Fe^{3+}, In^{3+}) have a suitable band, the photocatalysts do not work under visible light irradiation to directly decompose pure water, even CH_3OH/H_2O solution. Modification of the surface of the photocatalysts may be needed to increase responding wavelength range.

The lattice parameters decreased with decrease of M^{3+} ionic radii. However, the activity of the Bi_2MNbO_7 (M^{3+} = Fe^{3+}, In^{3+}) photocatalysts strongly increased with decrease of the M^{3+} ionic radii. Attempts to increase surface area of Bi_2MNbO_7 (M^{3+} = Fe^{3+}, In^{3+}) might increase activity of photocatalysts and increase responding wavelength range.

Although we could only demonstrate that there are some O_2 molecule photoadsorbed on surface of the photocatalysts and it is not clear whether the oxygen molecules are physisorbed and/or chemisorbed, we have shown that the localization of holes at the surface results in the formation of photoadsorbed oxygen molecules. The study of modification of structure by controlling the ionic radius in photocatalysts for improving the activity will provide useful information on the mechanism of photocatalysts and also on making the photocatalysts with high activity.

Acknowledgements

The authors would like to thank Dr. K. Sayama for his valuable discussion.

References

[1] T. Kawai, T. Sakata, Nature 286 (1980) 474.
[2] B.S. Geoffrey, E.M. Thomas, J. Phys. Chem. B 101 (1997) 2508.
[3] K. Yeong, S. Samer, J.H. Munir, E.M. Thomas, J. Am. Chem. Soc. 113 (1991) 9561.
[4] K. Sayama, K. Yase, H. Arakawa, K. Asakura, T. Tanaka, K. Domen, T. Onishi, J. Photochem. Photobiol. A 114 (1998) 125.
[5] L.L. Amy, L. Guangqan, T. John, J.T. Yates Jr., Chem. Rev. 95 (1995) 735.
[6] T. Takata, A. Tanaka, M. Hara, J. Kondo, K. Domen, Catal. Today 44 (1998) 17.
[7] A. Kudo, H. Kato, Chem. Lett. (1997) 867.
[8] K. Honda, A. Fujishima, Nature 238 (1972) 37.
[9] H.G. Kim, D.W. Hwang, J. Kim, Y.G. Kim, J. Lee, J. Chem. Commun. (1999) 1077.
[10] A. Kudo, K. Omiori, H. Kato, J. Am. Chem. Soc. 121 (1999) 11459.
[11] A. Kudo, H. Kato, S. Nakagawa, J. Phys. Chem. B 104 (2000) 571.
[12] Z. Zou, J. Ye, A. Abe, H. Arakawa, Catal. Lett. 68 (2000) 253.
[13] Z. Zou, J. Ye, K. Oka, Y. Nishihara, Phys. Rev. Lett. 80 (1998) 1074.
[14] E.A. Meulenkamp, A.R. Wrr, Electrochim. Acta 41 (1996) 109.
[15] F. Izumi, J. Crystallogr, Assoc. Jpn. 27 (1985) 23.
[16] D.E. Scaife, Solar Energy 25 (1980) 41.
[17] R.C. Alig, S.W. Bloom, Phys. Rev. B 22 (1980) 5565.
[18] J.I. Pankove, Optical Processes in Semiconductors, Dover, New York, 1970.
[19] S.M. Quinlan, P.J. Hirschfeld, D.J. Scalapino, Phys. Rev. B 53 (1996) 8575.
[20] D. Lawless, N. Serpone, D. Meisel, J. Phys. Chem. 95 (1991) 5166.
[21] S. Goldstein, G. Czapski, J. Rabani, J. Phys. Chem. 98 (1994) 6586.
[22] Y. Yanagisawa, Y. Ota, Surf. Sci. 254 (1991) L433.
[23] G. Lu, L. Amy, J.T. Yates Jr., J. Chem. Phys. 102 (1995) 3005.
[24] L.L. Amy, L. Guangqan, T. John, J.T. Yates Jr., Chem. Rev. 95 (1995) 435.
[25] K.-I. Ishibashi, A. Fijishima, T. Watanabe, K. Hashimoto, J. Phys. Chem. B 104 (2000) 4934.
[26] S. Gregory, Phys. Rev. Lett. 40 (1978) 723.
[27] V. Cannella, J.A. Mydosh, Phys. Rev. B 6 (1972) 4220.
[28] Z. Zou, J. Ye, Y. Nishihara, J. Mater. Sci. Lett. 18 (1999) 1387.
[29] J. Xu, M. Greenblatt, J. Solid State Chem. 121 (1996) 273.
[30] K. Matsuura, T. Wada, T. Nakamizo, H. Yamauchi, S. Tanaka, J. Solid State Chem. 94 (1991) 294.
[31] J. Xu, T. Emge, V.R. Ramanujachary, P. Hohn, M. Greenblatt, J. Solid State Chem. 125 (1996) 192.